Invariant Chain Transmembrane Domain Trimerization: A Step in MHC Class II Assembly†

Ann M. Dixon,‡,§ Bradford J. Stanley,‡ Erin E. Matthews,|| Jessica P. Dawson,‡,⊥ and Donald M. Engelman*,‡

Department of Molecular Biophysics and Biochemistry, Yale University, P.O. Box 208114, New Haven, Connecticut 06510, and Department of Chemistry, Yale University, New Haven, Connecticut 06510

Received October 17, 2005; Revised Manuscript Received January 13, 2006

ABSTRACT: The transmembrane (TM) domain of the major histocompatibility complex (MHC) class II-associated invariant chain (Ii) has long been implicated in both correct folding and function of the MHC class II complex. To function correctly, Ii must form a trimer, and the TM domain is one of the domains thought to stabilize the trimeric state. Specific mutations in the TM domain have been shown previously to disrupt MHC class II functions such as mature complex formation and antigen presentation, possibly due to disruption of Ii TM helix−helix interactions. Although this hypothesis has been reported several times in the literature, thus far no experimental measurements have been made to explore the relationship between TM domain structure and TM mutations that affect Ii function. We have applied biophysical and computational methods to study the folding and assembly of the Ii TM domain in isolation and find that the TM domain strongly self-associates. According to analytical ultracentrifugation analyses, the primary oligomeric state for this TM domain is a strongly associated trimer with a dissociation constant of approximately 120 nM in DPC micelles. We have also examined the effect of functionally important mutations of glutamine and threonine residues in the TM domain on its structure, providing results that now link the disruption of TM helix interactions to previously reported losses of Ii function.

The major histocompatibility complex (MHC)[1] class II-associated invariant chain (Ii) is a 216-residue membrane protein whose function is critical in the endosomal pathway for antigen presentation (*1*−*4*). Ii forms a homotrimer after biosynthesis (*5*, *6*) and subsequently binds three MHC class II α/β heterodimers (*7*, *8*) to form a nine-chain complex. Only as part of this nine-chain complex with Ii will class II molecules be released from the endoplasmic reticulum, protected from rapid degradation, and targeted to the endosomal pathway.

The correct assembly of Ii into its trimeric form is an essential first step in the endosomal pathway. Trimerization is thought to be mediated by two regions of Ii, a lumenal "trimerization" domain composed of residues 118−192 (*9*, *10*) and the transmembrane (TM) domain containing residues 30−56 (Figure 1a) (*11*). Structural evidence for trimerization has only been obtained conclusively for the lumenal trimerization domain (*9*, *10*, *12*, *13*), suggesting that this region dominates Ii self-association. However, recent studies are revealing the importance of the TM domain in Ii trimerization. Residues 1−80 of Ii have been shown to form trimers in the absence of the lumenal domain (*11*), suggesting the TM domain is a site of significant protein−protein interactions. Sequence alignment and functional data also suggest that the TM domain of Ii is important for its function. Not only is the sequence of this domain highly conserved across species (Figure 1b) (*14*), but mutations in the TM domain of Ii can lead to disrupted antigen presentation (*15*).

TM domain mutations may disrupt antigen presentation by destabilizing the Ii trimer. In support of this hypothesis, simultaneous mutation of a group of three polar residues in the TM domain (Gln47, Thr49, and Thr50; Figure 1b) was shown to prevent trimerization of full-length Ii and subsequent formation of the mature class II complex (*11*). These results stimulated a molecular dynamics (MD) simulation that predicted the association of α-helical TM domains from wild-type Ii into a left-handed coiled coil trimer containing a plausible hydrogen bonding network between Gln47 and Thr50 (*16*). The role of the Ii TM domain in trimer formation can be conceptualized using the "two-stage model" of membrane protein folding (*17*). According to the two-stage model, side-by-side interactions of TM α-helices in the plane of the bilayer determine the folding and assembly of membrane proteins. Studies of helix−helix interactions have revealed important sequence motifs, such as motifs of polar

† This work was supported by National Institutes of Health Grant GM54160 and American Cancer Society postdoctoral fellowship (A.M.D.) Grant PFCSM-0301701.

* To whom correspondence should be addressed. Telephone: (203) 432-5600. Fax: (203) 432-6381. E-mail: donald.engelman@yale.edu.

‡ Department of Molecular Biophysics and Biochemistry.

§ Current address: Department of Chemistry, University of Warwick, Coventry CV4 7AL, United Kingdom.

|| Department of Chemistry.

⊥ Current address: Department of Biochemistry and Biophysics, University of Pennsylvania School of Medicine, Philadelphia, Pennsylvania 19104.

[1] Abbreviations: TM, transmembrane; MHC, major histocompatibility complex; Ii, invariant chain; DPC, dodecylphosphocholine; MD, molecular dynamics; CD, circular dichroism; SDS, sodium dodecyl sulfate; C_8E_5, polyoxyethylene 9-lauryl ether; CAT, chloramphenicol acetyltransferase; rmsd, root-mean-square deviation; SDS−PAGE, sodium dodecyl sulfate−polyacrylamide gel electrophoresis; SRS, sum of residuals squared; SRV, square root of variance; DOF, degrees of freedom.

10.1021/bi052112e CCC: $33.50
Published on Web 03/29/2006

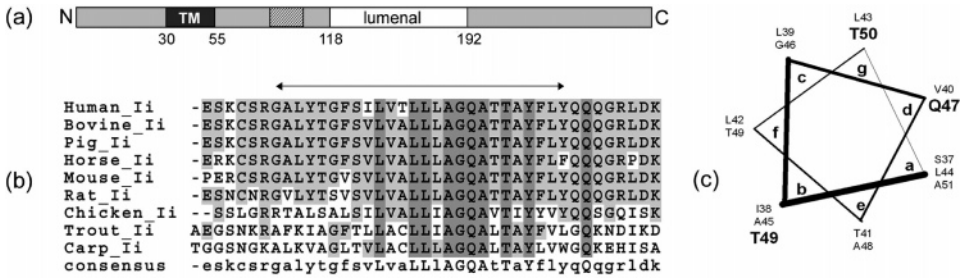

FIGURE 1: (a) Schematic diagram of human Ii depicting the transmembrane domain (black) and the lumenal trimerization domain (white). (b) Multiple-sequence alignment of nine Ii transmembrane domains, using ClustalW. The arrow indicates the location of TM residues 30−55. (c) Helical wheel plot of the human Ii TM domain highlighting in bold the positions of Gln47, Thr49, and Thr50, residues which when mutated yield a functionally deficient protein.

residues (*18*−*22*), that can drive specific association and stabilize TM helix oligomers. The predicted polar residue-driven folding of Ii TM domains is consistent with studies that show strong glutamine self-association in a lipid environment (*23*) and suggests that Gln47 in the TM domain of MHC Ii may facilitate trimer formation.

The mutagenesis and MD simulation data in previous studies point toward an important role for the TM domain in the functional assembly of Ii, but the structural implications of these studies remain unclear. To date, there has been no experimental evidence to confirm the role of the TM domain in Ii trimerization. Oligomerization has only been confirmed for an 80-residue region of Ii, a region that is in itself highly conserved among species (*14*) and therefore may contain other important features independent of the TM. Furthermore, although a group of polar residues in the TM domain has been shown to disrupt trimerization of full-length Ii, the mechanism of disruption is not fully understood since all mutations were made simultaneously.

To unambiguously address the role of the TM domain in Ii trimerization, we have isolated the TM domain from the rest of the protein. Analytical ultracentrifugation and chemical cross-linking were used to examine the assembly, stoichiometry, and binding energy of the wild-type Ii TM domain in a variety of detergents. Additionally, to more clearly assess the structural effects of key mutations known to disrupt Ii function, we have investigated these mutations one at a time using the TOXCAT assay, which measures the degree of oligomerization of α-helical TM domains in the inner membrane of *Escherichia coli* (*24*). Finally, molecular models were used to illustrate likely points of contact in oligomers of wild-type Ii TM and several mutants. These models and the experimental data support a single, specific mechanism of interaction that drives trimer formation in the Ii TM domain. This work confirms for the first time the oligomeric state of the Ii TM domain and provides structural data that move us closer to an understanding of the relationships among sequence, structure, and function in the MHC class II complex.

MATERIALS AND METHODS

Peptide Sequence and Purification. A peptide corresponding to the TM and juxtamembrane domains of human MHC Ii (Ii_{TM}) was synthesized by the Keck Facility at Yale University using F-moc chemistry. The sequence of the Ii_{TM} peptide was KASRGALYTGFSILVTLLLAGQATTAY-FLYQQQGR, containing residues K26−R60 from Ii. Purification of Ii_{TM} was achieved using reversed-phase high-pressure liquid chromatography with a linear gradient to a final solvent composition of 95% (v/v) acetonitrile. Pooled fractions were lyophilized, and the molecular weight and purity of the product were confirmed using mass spectrometry.

Circular Dichroism. Circular dichroism (CD) measurements were taken at 25 °C using an Aviv model 215 CD spectrophotometer with a 0.1 cm path length. CD spectra were collected from 190 to 260 nm on samples prepared in 50 mM sodium phosphate buffer (pH 7.5) containing 150 mM sodium chloride as well as detergent for solubilization. Peptide concentrations were estimated using a molar extinction coefficient (ϵ) at 280 nm of 4470 mol^{-1} cm^{-1}. Measurements were carried out on samples containing 50 μM Ii_{TM} peptide and either (a) 10 mM sodium dodecyl sulfate (SDS), (b) 15 mM dodecylphosphocholine (DPC), or (c) 70 mM polyoxyethylene 9-lauryl ether (C_8E_5). For samples containing peptide, four individual spectra were averaged, and a spectrum of the detergent in buffer was subtracted to obtain the final spectrum.

Peptide Cross-Linking in Detergents. Cross-linking reactions were carried out in 50 mM sodium phosphate buffer (pH 7.5) containing either (a) 15 mM DPC, (b) 30 mM C_8E_5, or (c) 10 mM SDS. Concentrations of the Ii_{TM} peptide ranged from 9.4 to 76 μM. Glutaraldehyde was used to cross-link the peptide in solution via primary amine groups according to a reported protocol (*25*). Quenching was allowed to proceed for a minimum of 10 min before an aliquot of the reaction mixture was removed for analysis by gel electrophoresis. Visualization of the peptide on gels was achieved by staining with either Coomassie blue or the Silver Stain Plus system (Bio-Rad, Hercules, CA).

Analytical Ultracentrifugation of Ii_{TM} in Detergents. Sedimentation equilibrium experiments were performed on a Beckman XL-I analytical ultracentrifuge at 25 °C. Scans of absorbance at 280 nm versus radius were taken in carbon-epoxy six-sector cells. Data were collected at three Ii_{TM} peptide concentrations and at three speeds: 40 000, 48 000, and 60 000 rpm. Samples were centrifuged for time periods in excess of those required to reach equilibrium (20 h per speed), and the establishment of a sedimentation equilibrium was verified at each speed using Win Match to subtract successive scans until no difference was observed. Experiments were performed in buffers that matched the buoyant density of the detergent in the sample. When the solvent matches the buoyant density of the detergent micelles, the only contribution to the buoyant molecular weight is from the peptide, as described previously (*26*). The first buffer

contained 50 mM sodium phosphate (pH 7.5), 150 mM sodium chloride, and 70 mM C_8E_5. The detergent C_8E_5 has a micellar buoyant density of 0.999, so the solvent density was not adjusted (*27*). In this buffer, Ii_{TM} peptide concentrations ranging from 22 to 80 μM were analyzed. Because of the low solubility of Ii_{TM} in C_8E_5, a second buffer was used which contained 15 mM DPC, 50 mM Tris (pH 7.4), 100 mM sodium chloride, and 52.5% D_2O to match the buoyant density of the detergent. In the buffer containing DPC, peptide concentrations ranging from 50 to 160 μM were readily analyzed. Buffers containing SDS cannot be density matched using D_2O due to the high density of the detergent; therefore, SDS was not used in these analyses. The peptide monomer molecular mass and partial specific volume in 52.5% D_2O were determined to be 3876.2 Da and 0.7496, respectively, using SEDNTERP (*28*). Data collected at an absorbance of 280 nm were analyzed by nonlinear least-squares curve fitting using Win-NONLIN (*29*). Global fitting of the nine resulting data sets, i.e., data at three speeds and three concentrations, was performed to determine a single, global association constant per model.

TOXCAT Assay and Construction of Chimera. Interaction of the Ii TM domain and mutants of interest in a natural membrane was investigated using the TOXCAT assay, the details of which have been described previously (*24*). Briefly, TOXCAT employs a chimeric protein in which the α-helical TM domain of interest is inserted between the N-terminal DNA binding domain of ToxR, a dimerization-dependent transcriptional activator, and maltose binding protein (MBP), a monomeric periplasmic anchor protein. The fusion protein is constitutively expressed in *E. coli* together with a chloramphenicol acetyltransferase (CAT) reporter gene under the control of a ToxR-responsive *ctx* promoter. Oligomerization of the TM domains within the bacterial inner membrane results in oligomerization of the ToxR domain, transcriptional activation of the *ctx* promoter, and CAT expression. The amount of CAT expressed in this system is proportional to the strength of oligomerization of the TM domains. TOXCAT chimera were constructed according to a reported protocol (*24*) and expressed in *E. coli*. Before the assay was performed, membrane insertion of all constructs was confirmed using sodium hydroxide washes (*30*), and the correct orientation of the TOXCAT constructs in the membrane was confirmed through protease sensitivity in a spheroplast assay (*24*). Similar expression levels for all constructs were confirmed via Western analysis against the MBP domain prior to performing CAT assays. The CAT assays were performed using the Quant-T-CAT kit (Amersham, Piscataway, NJ) as described previously (*24*).

Computational Searches Using CHI. Structural calculations were carried out using the CNS searching of helix interactions (CHI) method, the details of which have been described previously (*31*−*33*). All structural calculations were carried out in vacuo on a Silicon Graphics O2 workstation. Using CHI, three canonical α-helices containing residues A31−Y55 of Ii and its mutants were built. The starting geometries incorporated both right-handed (−25°) and left-handed (25°) crossing angles and an axis-to-axis distance between the three helices ranging from 10 to 11.0 Å. In a search of approximately symmetrical interactions, the three helices were simultaneously rotated about their central axis in 10° increments from 0 to 360°. Molecular dynamics (MD) simulations were performed using simulated annealing of atomic coordinates after each rotation. Four different MD simulations were performed for each starting geometry, and energy minimization of structures was carried out both before and after MD simulations. Groups of structures with a backbone rmsd of ≤1 Å were placed into clusters of 10 or more members, followed by calculation of an average structure for each cluster and energy minimization.

RESULTS AND DISCUSSION

Secondary Structure in a Variety of Detergents. To work with the TM domain of Ii outside of a membrane bilayer, the α-helical secondary structure must be reproduced. To determine the secondary structure of the Ii TM domain in a range of detergents, CD spectra were collected for the detergent-solubilized Ii_{TM} peptide (results not shown). Measurements were carried out in three detergents with differing chemical properties: (a) SDS, an anionic and denaturing detergent; (b) DPC, a zwitterionic detergent thought to be less denaturing than SDS; and (c) C_8E_5, a neutral and nondenaturing detergent. In each case, the CD spectra show characteristic absorption minima at 208 and 220 nm, confirming that the Ii_{TM} peptide is α-helical in all three detergents.

Oligomeric State of the Ii TM Domain. Although the TM domain of Ii has been predicted to form trimers and an 80-residue truncated version of the protein (containing the TM domain) has been shown to trimerize (*11*, *16*), there are as yet no data that measure the oligomeric state of the Ii TM domain. To investigate oligomerization of the Ii TM domain and therefore unambiguously address the question of whether it contributes to trimer formation, the Ii_{TM} peptide was analyzed using sodium dodecyl sulfate−polyacrylamide gel electrophoresis (SDS−PAGE). Initially, the peptide was solubilized in SDS detergent and analyzed. This resulted in a predominantly monomeric species for the Ii_{TM} peptide. Given that SDS, a highly denaturing detergent, has been shown to destabilize transmembrane oligomer formation relative to zwitterionic detergents (*34*), this result did not rule out assembly in a lipid environment or less denaturing detergents.

The oligomeric state of Ii_{TM} was investigated in less denaturing detergents by means of chemical cross-linking. Glutaraldehyde, a homo-bifunctional amine reactive cross-linking agent, was added to various concentrations of Ii_{TM} solubilized in either DPC or C_8E_5 micelles. The cross-linked peptides were then analyzed by SDS−PAGE (Figure 2). As a negative control, cross-linking was also performed on samples dissolved in SDS (Figure 2a). A ladder of Ii_{TM} oligomers formed in both DPC and C_8E_5 detergents, beginning with trimer, and including hexamer, nonamer, and higher-order oligomers. A prominent feature of the cross-linking results is that, in the less denaturing DPC and C_8E_5 detergents, the trimer is the predominant species. These results provide the first evidence that the Ii TM domain forms trimers.

To probe the ability of wild-type Ii_{TM} to self-associate in the absence of a cross-linker, sedimentation equilibrium analytical ultracentrifugation measurements were performed for the DPC-solubilized peptide. The concentration versus

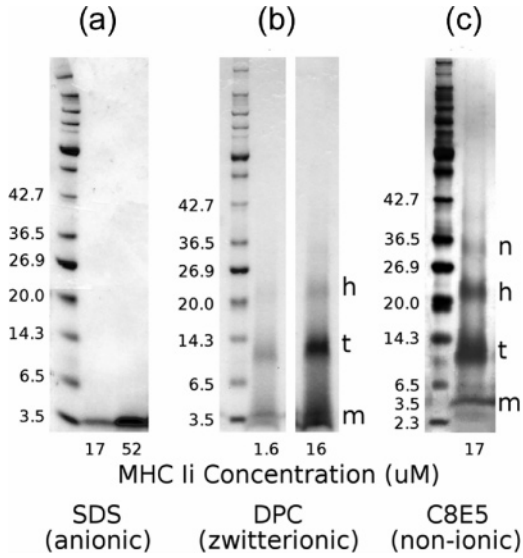

FIGURE 2: SDS−PAGE results for the glutaraldehyde cross-linked Ii_{TM} peptide in (a) 10 mM SDS, (b) 15 mM DPC, and (c) 30 mM C_8E_5. Gels shown in panels a and b were stained using Coomassie blue. Because of the low solubility of the Ii_{TM} peptide in C_8E_5, silver staining was required to visualize the peptide in panel c. The far left lanes in each figure display molecular weight markers, and multiple lanes indicate results at increasing peptide concentrations. The oligomeric state of the Ii_{TM} peptide is indicated at the right by m (monomer), t (trimer), h (hexamer), or n (nonamer).

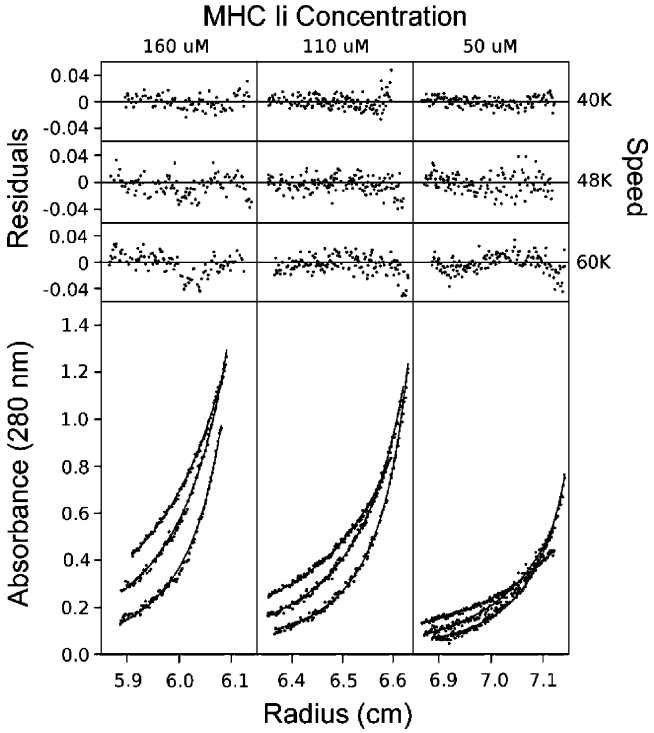

FIGURE 3: Sedimentation equilibrium data for the Ii_{TM} peptide in 15 mM DPC. Shown in the three bottom plots are the data collected at three concentrations, ranging from 50 to 160 μM. At each concentration, data were collected at three speeds, 40 000, 48 000, and 60 000 rpm. Filled circles represent experimental data, and solid curves display the best fit resulting from global analysis of all nine data sets, in this case the fit of a model representing a monomer−trimer equilibrium. Above each plot are the residuals of the fit to the data at each speed.

radial distance profiles collected for Ii_{TM} in DPC at three concentrations and three speeds are shown in Figure 3. Data were initially fit to a monomer model, followed by fitting to models of increasing complexity as described previously (*27*), until the variance was minimized and the randomness of the fit residuals was optimized. The fitting statistics from each of the data analyses are summarized in Table 1 and indicate the data fit best to a monomer−trimer model in DPC. Residuals from global fitting of the data to a single monomer−trimer dissociation constant are given in Figure 3. Although this fit produced the most random residuals, the linearity of the residuals decreases with an increase in speed, indicating that the fit algorithm may not be precisely representing the higher-order species present in the sample. The fit yielded an apparent monomer−trimer dissociation constant of 127 nM in 15 mM DPC and a corresponding free energy of dissociation (ΔG_d) of 9.4 kcal/mol at 25 °C, indicating that the trimer is the strongest and most abundant oligomeric state in DPC detergent. These results, in agreement with cross-linking results, confirm for the first time that the α-helical Ii TM domain forms trimers.

Table 1: Nonlinear Least-Squares Fitting Statistics[a] for Sedimentation Equilibrium Data and Resulting Dissociation Constants[b] for the Ii_{TM} Peptide

					K_d (M)	
fit	variance	SRS	SRV	DOF	dimer	trimer
M	6.89×10^{-4}	0.764	2.62×10^{-2}	1111	−	−
M−D	1.93×10^{-4}	0.213	1.38×10^{-2}	1110	0.353	−
M−T	1.50×10^{-4}	0.160	1.22×10^{-2}	1110	−	1.27×10^{-7}
M−D−T	1.96×10^{-4}	0.217	1.40×10^{-2}	1109	0.383	1.24×10^{-7}

[a] Statistics are given for fits to monomer (M), monomer−dimer (M−D), monomer−trimer (M−T), and monomer−dimer−trimer (M−D−T) equilibria. The variance of fit, the sum of residuals squared (SRS), the square root of variance (SRV), and the number of degrees of freedom (DOF) in the fit are given. [b] Also shown are the apparent dissociation constants (K_d) as calculated from the fits for both the dimer and trimer.

Also shown in Table 1 are the results from fits to monomer−dimer and monomer−dimer−trimer equilibria. Although these models do not describe the data as well as the monomer−trimer model, alterations in the model appear to produce little or no change in either the monomer−dimer or monomer−trimer dissociation constants. When the dimer was included in the fit, only weak dimerization of Ii_{TM} in 15 mM DPC resulted, yielding a monomer−dimer dissociation constant of approximately 300 mM and a free energy of dissociation (ΔG_d) of 0.6 kcal/mol at 25 °C. Similar weak dimerization in concert with strong trimerization is observed for full-length Ii (*11*), revealing an interesting correlation between the oligomerization behavior of the Ii_{TM} domain and that of the full-length protein and raising the possibility that Ii trimerization may be initiated and/or regulated by its TM domain.

Effect of Functionally Disruptive Mutations on Ii TM Domain Association. Mutation of the TM domain of Ii has been shown in previous studies to disrupt functions such as mature complex formation and antigen presentation (*11*, *15*). This effect was traced to a group of polar residues in the TM domain (Gln47, Thr49, and Thr50) which, when mutated, abolished trimerization of Ii (*11*), and it was proposed that the mutations specifically decreased the efficiency of interactions between Ii TM domains; however, this hypothesis has yet to be confirmed.

Examination of the residues in the triple mutant using sequence alignment of several Ii TM domains (Figure 1b)

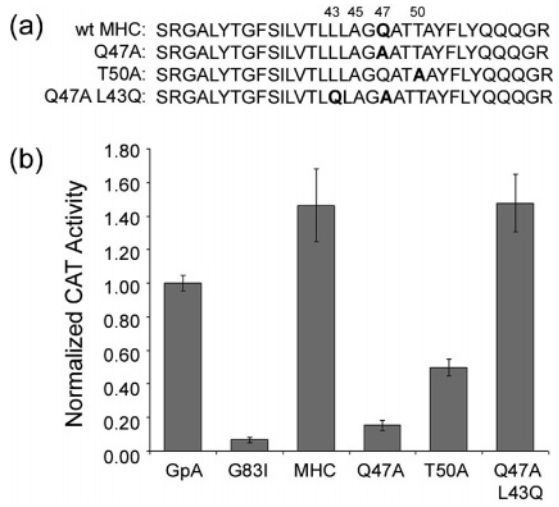

FIGURE 4: (a) Sequences of the wild-type Ii transmembrane domain (residues S_{28}−R_{60}) and three mutants of interest, with the positions of mutation listed above the sequences. The resulting CAT activities obtained from the TOXCAT assay are shown in panel b, along with data from glycophorin A (GpA) and its dimerization-defective mutant G_{83}I as positive and negative controls, respectively. All values for CAT activity are normalized to that of GpA.

as well as a helical wheel plot of the human Ii TM domain (Figure 1c) reveals that two of the three residues, namely, Gln47 and Thr50, are entirely conserved and lie on the same face of the TM helix. Thr49 lies on the face of the helix opposite Gln47 and Thr50 and is not as highly conserved in the TM domain sequence, indicating that it is less likely to participate in TM helix interactions. Using these results as well as existing knowledge of the roles of Gln and Thr in TM helix associations (*20*, *21*) as a guide, our investigation was focused on Gln47 and Thr50. To determine the role of Gln47 and Thr50 in Ii TM domain association, the TOXCAT assay was used.

Although TOXCAT does not provide a measure of the order of the oligomers that formed, it is a powerful tool for assessing the relative strength of TM helix interactions in a natural membrane bilayer. Mutations were introduced to address the effects of removing Gln47, removing Thr50, and altering the position of these residues relative to one another. The TOXCAT data, along with the sequences of the wild-type Ii TM domain and all mutants investigated, are shown in Figure 4. Comparison of the wild-type Ii TM TOXCAT signal to that of GpA indicates that, in agreement with cross-linking and sedimentation equilibrium results, the Ii TM domain forms strong homo-oligomers in the membrane. As predicted, the greatest disruption in oligomerization was seen when the Gln47 residue was removed and replaced with Ala (Q47A). The Q47A mutation produced a 90% drop in CAT activity, confirming that Gln47 plays a major role in the association of Ii TM domains. The removal of Thr50 also had a significant effect on the association of the Ii TM domain. Mutation of Thr50 to Ala (T50A) resulted in a 65% drop in CAT activity, demonstrating that, although its effect on oligomerization is not as great as that of Gln47, Thr50 does play a significant role in stabilizing interactions between TM domains.

These TOXCAT results show that Gln47 and Thr50 each contribute to association of the Ii TM domain; however, the nature of the interactions was unclear. Previous MD simulations predicted that Gln47 and Thr50 form a network of hydrogen bonds involving both residues (*16*). To investigate this experimentally, the Gln residue was moved to position 43 (Q47A/L43Q), placing it one complete turn of the helix deeper into the membrane and two turns (as opposed to one in the wild type) away from Thr50, thus preventing any hydrogen bonding between Gln47 and Thr50. If the predictions are correct, we should see a large drop in CAT activity. Surprisingly, no decrease in CAT activity was observed for this mutation, demonstrating that Gln47 and Thr50 work independently to stabilize TM domain interactions.

Ii TM domain associations have been shown here to be predominantly mediated by highly conserved Gln and Thr residues that lie on the same face of the TM helix. These residues act independently, and not in concert as once predicted, to stabilize the TM helix oligomer. Most importantly, these data link specific mutations in the Ii TM domain, mutations that have been previously reported to abolish functions such as mature complex formation and antigen presentation, with the weakening of TM helix−helix interactions, a result that suggests the possible importance of the Ii TM domain in MHC class II function.

Structural Effects of TM Domain Mutations. The results presented herein establish that the Ii TM domain can associate to form trimers and that mutation of Gln and Thr residues in the TM domain disrupts this association. To gain insight into structural features of the wild-type Ii TM domain trimer as well as the impact of specific mutations on its structure, we produced computational models using CHI (see Materials and Methods). CHI searches were performed on three parallel α-helices containing either the sequence of the Ii TM domain or those of the three mutants. The trimer models suggest that each of the TM domains can form a chemically plausible left-handed coiled coil, in agreement with the previous model of the wild-type Ii TM (*16*). In all of the models (Figure 5), the interaction interface is composed of residues at positions 36, 37, 40, 43, 47, and 50, positions that are highly conserved in the Ii TM domain (Figure 1b) and fall on the same face of the helix (Figure 1c).

In the model of the wild-type Ii TM domain trimer, both Gln47 and Thr50 could contribute interhelical hydrogen bonds. Hydrogen bonds were assigned in these analyses whenever a hydrogen bond donor and acceptor were within 3 Å of one another. As shown in Figure 5, the highly polar amide groups on the side chains of all three Gln47 residues could form hydrogen bonds to the carbonyl oxygen of glycine 46 on a separate helix. Thr50 could form a single interhelical hydrogen bond to another Thr50 side chain on a separate monomer. It is apparent in this model that the interactions of Gln47 and Thr50 are quite separate from one another, as has also been demonstrated using the TOXCAT assay. We suggest that this model is a more accurate representation of our experimental data and that, although both Gln47 and Thr50 can contribute to associations, no hydrogen bonding network is formed between the two.

It follows from the model of the wild-type Ii TM trimer that, upon removal of Gln47, we should observe a large disruption of TM helix interactions as we remove most of the plausible interhelical hydrogen bonds. This disruption is observed experimentally in the TOXCAT data, and it is also illustrated in the model for the Q47A trimer (Figure 5).

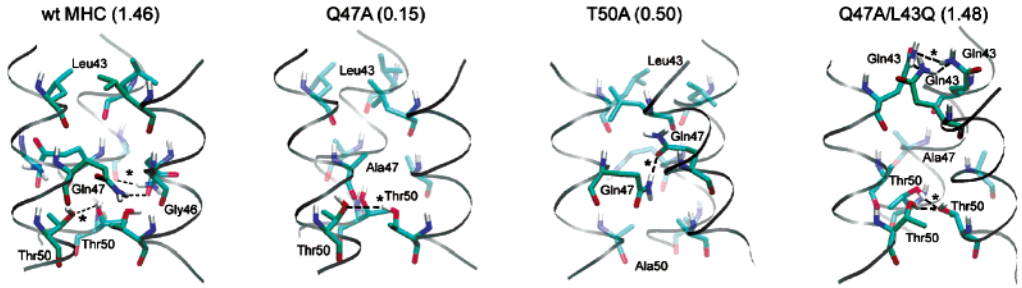

FIGURE 5: Structural models of left-handed trimers of wild-type Ii TM and the three TOXCAT mutants calculated using CHI. Above each structure are given the nature of the mutation and the corresponding CAT activity (in parentheses). Predicted interhelical hydrogen bonds are represented by dashed lines as well as asterisks.

Replacement of Gln47 with an alanine residue prevents any hydrogen bond formation at this position, leaving only a single potential interhelical hydrogen bond via Thr50. A weaker effect was expected upon mutation of Thr50 to Ala, as only one of the four interhelical hydrogen bonds would be lost, but surprisingly, the TOXCAT data showed a 65% drop in CAT activity for the T50A mutant. The model clarifies this result to some extent (Figure 5) as we see that in the T50A mutant, Gln47 would contribute only one interhelical hydrogen bond instead of three. One possible explanation for this result is that Thr50 may not only contribute to TM helix interactions through formation of an interhelical hydrogen bond but also help to optimally align the oligomer for maximum hydrogen bonding of Gln47 residues in the trimer.

Finally, a model was created for the Q47A/L43Q mutant to verify that the helix−helix interactions could involve the same polar resides as in the wild type. As shown in Figure 5, the model indicates that both Gln43 and Thr50 could form multiple interhelical hydrogen bonds. It appears that the distance between these residues is not important in the stabilization of helix interactions, as demonstrated several times herein. It seems more important that the Gln and Thr residues appear on the same face of the helix.

The trimer structural models are consistent with the results obtained using TOXCAT and support a mechanism of TM helix association predominantly stabilized by interhelical hydrogen bonding of the strongly polar amide groups on glutamine side chains. Although we see no evidence of the formation of a hydrogen bonding network between Gln47 and Thr50, as previously suggested (*16*), additional independent interactions of Thr50 residues could clearly increase the stability of the TM oligomers. Most importantly, these models illustrate how the functionally significant mutations of Gln47 and Thr50 in the Ii TM domain reported by Ashman and Miller (*11*) strongly affect TM helix interactions, linking the functional assembly of this protein to the transmembrane domain structure.

CONCLUSIONS

The transmembrane domain of Ii has long been suspected of playing an important role in the assembly of the protein into trimers. Specific residues in the TM domain, namely, Gln47 and Thr50, have been shown to be crucial in the functional assembly of the MHC II complex, possibly by stabilizing transmembrane helix−helix interactions. Despite these data, there was no experimental evidence evaluating the ability of the Ii TM domain to self-associate or the

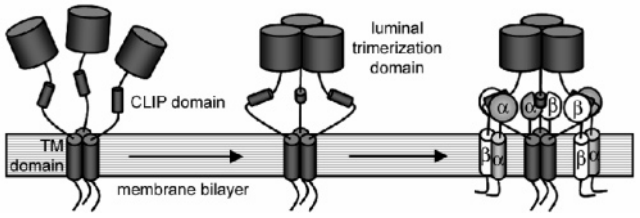

FIGURE 6: Revised model for MHC class II complex assembly, accounting for the strong TM domain associations reported in this work. In this model, we suggest the possibility that trimerization of Ii is initiated by the transmembrane domain and is followed by trimerization of the lumenal trimerization domain. After the Ii trimer is formed, three α/β MHC class II heterodimers bind to the CLIP domain of Ii to form the mature complex.

structural impact of the functionally important mutations. The work presented here has directly addressed both points. It has now been shown that the TM domain of Ii strongly self-associates into trimers in the absence of any other regions of the protein, with an approximate $\Delta G_{d,25°C}$ of 9.4 kcal/mol, and it also appears to form weak dimers. In this way, the TM domain reflects the oligomerization behavior of the full-length protein. The Ii TM has also been shown here to have a polar residue-mediated mechanism of helix−helix association, with the polar glutamine residue (Gln47) located at the center of the TM domain dominating the interaction. Our models suggest this occurs by means of interhelical hydrogen bonding of amide groups on Gln47. The helix interactions may be further stabilized by independent hydrogen bonding of Thr50, a residue that also appears to help maximize hydrogen bonding in Gln47.

Incorporation of our results into the current model of mature MHC class II complex formation (*35*, *36*) yielded the revised model given in Figure 6. This model differs from previous models in that Ii trimer formation is initiated by the TM domain, not the lumenal trimerization domain. Although we do not dispute the fact that the lumenal domain forms trimers, without a dissociation constant for trimerization of this domain it is difficult to assess the relative contribution to Ii oligomerization. It has already been reported that Ii trimerization is abolished by mutations in the TM domain (*11*) despite the lumenal domain remaining intact, a result that is difficult to explain if the lumenal domain is thought to drive trimerization. Our revised model explains a possible mechanism by which mutation of Gln47 and Thr50 in the TM domain results in the reported loss of function. We suggest that removal of these two key polar residues weakens TM helix−helix interactions and results in a decreased level of Ii oligomerization and therefore a less mature complex, which would in turn have a profound

effect on antigen presentation. Therefore, study of the TM domain of Ii has resulted in a model which may allow us to better relate interactions in the Ii TM domain to functional assembly of the MHC class II complex.

ACKNOWLEDGMENT

We thank J. Crawford for peptide synthesis, Professor L. Regan for the use of the circular dichroism spectrophotometer, and Dr. A. R. Curran and Dr. J. N. Sachs and for helpful discussions and critical reading of the manuscript.

REFERENCES

1. Germain, R. N., and Rinker, A. G. J. (1993) Peptide binding inhibits protein aggregation of invariant-chain free class II dimers and promotes surface expression of occupied molecules, *Nature 363*, 725−728.
2. Peterson, M., and Miller, J. (1992) Antigen presentation enhanced by the alternatively spliced invariant chain gene product p41, *Nature 357*, 596−598.
3. Romagnoli, P., Layet, C., Yewdell, J., Bakke, O., and Germain, R. N. (1993) Relationship between invariant chain expression and major histocompatibility complex class II transport into early and late endocytic compartments, *J. Exp. Med. 177*, 583−596.
4. Simonsen, A., Momburg, F., Drexler, J., Hammerling, J. H., and Bakke, O. (1993) Intracellular distribution of the MHC class II molecules and the associated invariant chain (Ii) in different cell lines, *Int. Immunol. 5*, 903−917.
5. Lamb, L. A., and Cresswell, P. (1992) Assembly and transport properties of invariant chain trimers and HLA-DR invariant chain complexes, *J. Immunol. 148*, 3478−3482.
6. Marks, M. S., Blum, J. S., and Cresswell, P. (1990) Invariant chain trimers are sequestered in the rough endoplasmic reticulum in the absence of association with HLA class II antigens, *J. Cell Biol. 111*, 839−845.
7. Kvist, S., Wiman, K., Claesson, L., Peterson, P. A., and Dobberstein, B. (1982) Membrane insertion and oligomeric assembly of HLA-DR histocompatibility antigens, *Cell 29*, 61−69.
8. Sung, E., and Jones, P. P. (1981) The invariant chain of murine Ia antigens: Its glycosylation, abundance and subcellular localization, *Mol. Immunol. 18*, 899−913.
9. Bijlmakers, M. E., Benaroch, P., and Ploegh, H. L. (1994) Mapping functional regions in the lumenal domain of the class II-associated invariant chain, *J. Exp. Med. 180*, 623−629.
10. Jasanoff, A., Wagner, G., and Wiley, D. C. (1998) Structure of a trimeric domain of the MHC class II-associated chaperonin and targeting protein Ii, *EMBO J. 17*, 6812−6818.
11. Ashman, J. B., and Miller, J. (1999) A role for the transmembrane domain in the trimerization of the MHC class II-associated invariant chain, *J. Immunol. 163*, 2704−2712.
12. Bertolino, P., Staschewski, M., Trescol-Biemont, M., Freisewinkel, I. M., Schenk, K., Chretien, I., Forquet, F., Gerlier, D., Rabourdin-Combe, C., and Koch, N. (1995) Deletion of a C-terminal sequence of the class II-associated invariant chain abrogates invariant chains oligomer formation and class II antigen presentation, *J. Immunol. 154*, 5620−5629.
13. Gedde-Dahl, M., Freisewinkel, I., Staschewski, M., Schenck, K., Koch, N., and Bakke, O. (1997) Exon 6 is essential for invariant chain trimerization and induction of large endosomal structures, *J. Biol. Chem. 272*, 8281−8287.
14. Bremnes, B., Rode, M., Gedde-Dahl, M., Nordeng, T. W., Jacobsen, J., Ness, S. A., and Bakke, O. (2000) The MHC Class II-Associated Chicken Invariant Chain Shares Functional Properties with its Mammalian Homologs, *Exp. Cell Res. 259*, 360−369.
15. Frauwirth, K., and Shastri, N. (2001) Mutation of the Invariant Chain Transmembrane Region Inhibits Ii Degradation, Prolongs Association with MHC Class II, and Selectively Disrupts Antigen Presentation, *Cell. Immunol. 209*, 97−108.
16. Kukol, A., Torres, J., and Arkin, I. T. (2002) A structure for the trimeric MHC class II-associated invariant chain transmembrane domain, *J. Mol. Biol. 320*, 1109−1117.
17. Popot, J. L., and Engelman, D. M. (1990) Membrane protein folding and oligomerization: The two-stage model, *Biochemistry 29*, 4031−4037.
18. Choma, C., Gratkowski, H., Lear, J. D., and DeGrado, W. F. (2001) Asparagine-mediated self-associated of a model transmembrane helix, *Proc. Natl. Acad. Sci. U.S.A. 98*, 880−885.
19. Dawson, J. P., Melnyk, R. A., Deber, C. M., and Engelman, D. M. (2003) Sequence context strongly modulates association of polar residues in transmembrane helices, *J. Mol. Biol. 331*, 255−262.
20. Dawson, J. P., Weinger, J. S., and Engelman, D. M. (2002) Motifs of serine and threonine can drive association of transmembrane helices, *J. Mol. Biol. 316*, 799−805.
21. Gratkowski, H., Lear, J. D., and DeGrado, W. F. (2001) Polar side chains drive the association of model transmembrane peptides, *Proc. Natl. Acad. Sci. U.S.A. 98*, 880−885.
22. Zhou, F. X., Merianos, H. J., Brunger, A. T., and Engelman, D. M. (2001) Polar residues drive association of polyleucine transmembrane helices, *Proc. Natl. Acad. Sci. U.S.A. 98*, 2250−2255.
23. Freeman-Cook, L. L., Dixon, A. M., Frank, J. B., Xia, Y., Ely, L., Gerstein, M., Engelman, D. M., and DiMaio, D. (2004) Selection and characterization of small random transmembrane proteins that bind and activate the platelet-derived growth factor β receptor, *J. Mol. Biol. 338*, 907−920.
24. Russ, W. P., and Engelman, D. M. (1999) TOXCAT: A measure of transmembrane helix association in a biological membrane, *Proc. Natl. Acad. Sci. U.S.A. 96*, 863−868.
25. Maduke, M., Pheasant, D. J., and Miller, C. (1999) High-level expression, functional reconstitution, and quarternary structure of a prokaryotic CIC-type chloride channel, *J. Gen. Physiol. 114*, 713−722.
26. Kochendoerfer, G. G., Salom, D., Lear, J. D., Wilk-Orescan, R., Kent, S. B., and DeGrado, W. F. (1999) Total chemical synthesis of the integral membrane protein influenza A virus M2: Role of its C-terminal domain in tetramer assembly, *Biochemistry 38*, 11905−11913.
27. Fleming, K. G., Ackerman, A. L., and Engelman, D. M. (1997) The effect of point mutations on the free energy of transmembrane α-helix dimerization, *J. Mol. Biol. 272*, 266−275.
28. Laue, T. M., Shah, B. D., Ridgeway, T. M., and Pelletier, S. L. (1992) Computer-aided interpretation of analytical sedimentation data for proteins, in *Analytical Ultracentrifugation in Biochemistry and Polymer Science* (Harding, S. E., Rowe, A. J., and Horton, J. C., Eds.) pp 90−125, The Royal Society of Chemistry, Cambridge, U.K.
29. Johnson, M. L., Correia, J. J., Yphantis, D. A., and Halvorson, H. R. (1981) Analysis of data from the analytical ultracentrifuge by nonlinear least-squares techniques, *Biophys. J. 36*, 575−588.
30. Chen, H., and Kendall, D. A. (1995) Artificial transmembrane segments. Requirements for stop transfer and polypeptide orientation, *J. Biol. Chem. 270*, 14115−14122.
31. Adams, P. D., Arkin, I. T., Engelman, D. M., and Brunger, A. T. (1995) Computational searching and mutagenesis suggest a structure for the pentameric transmembrane domain of phospholamban, *Nat. Struct. Biol. 2*, 154−162.
32. Adams, P. D., Engelman, D. M., and Brunger, A. T. (1996) Improved prediction for the structure of the dimeric transmembrane domain of glycophorin A obtained through global searching, *Proteins 26*, 257−261.
33. Brunger, A. T., Adams, P. D., Clore, G. M., DeLano, W. L., Gros, P., Grosse-Kunstleve, R. W., Jiang, J. S., Kuszewski, J., Nilges, M., Pannu, N. S., Read, R. J., Rice, L. M., Simonson, T., and Warren, G. L. (1998) Crystallography & NMR system: A new software suite for macromolecular structure determination, *Acta Crystallogr. D54*, 905−921.
34. Fisher, L. E., Engelman, D. M., and Sturgis, J. N. (2003) Effect of detergents on the association of the glycophorin A transmembrane helix, *Biophys. J. 85*, 3097−3105.
35. Cresswell, P. (1996) Invariant chain structure and MHC class II function, *Cell 84*, 505−507.
36. Jasanoff, A., Song, S., Dinner, A. R., Wagner, G., and Wiley, D. C. (1999) One of two unstructured domains of Ii becomes ordered in complexes with MHC class II molecules, *Immunity 10*, 761−768.

BI052112E